

**H.B. Kulynych, S.B. Herashchenko, V.M. Pertsovych, M. D. Ryzuk, I. Y. Oliynyk<sup>1</sup>, O.I. Tiron<sup>2</sup>**

**Ivano-Frankivsk National Medical University, Ivano-Frankivsk,**

**<sup>1</sup>Bukovina State Medical University, Chernivtsi,**

**<sup>2</sup>International Academy of Ecology and Medicine, Kyiv**

**ELECTRON MICROSCOPIC CHARACTERIZATION OF THE DYNAMICS OF SCIATIC NERVE DAMAGE IN RATS WITH CISPLATIN- AND PACLITAXEL-INDUCED NEUROTOXICITY**

e-mail: galija1979@ukr.net

Chemotherapy-induced peripheral neuropathy limits the efficacy of cisplatin and paclitaxel in cancer treatment. This study characterized ultrastructural changes in the rat sciatic nerve on days 14 and 28 post-administration using transmission electron microscopy. Adult male inbred rats (n=30/group) were divided into three groups: paclitaxel (2 mg/kg i.p., 4 injections every other day, total 8 mg/kg), cisplatin (2 mg/kg i.p., twice weekly for 4 weeks, total 16 mg/kg), and combined treatment (cisplatin 2 mg/kg i.p. at 37°C+paclitaxel 5 mg/kg i.v. weekly for 6 weeks; total cisplatin 12 mg/kg, paclitaxel 30 mg/kg). Nerve fragments were fixed in 2% osmium tetroxide, embedded in Epon/Araldite, and examined at  $\times 4800$ – $\times 16000$ . Cisplatin induced more severe degeneration than paclitaxel, including myelin destruction, axonal degeneration, and neuroglio-vascular swelling. Damage progressed from day 14 to 28, revealing cumulative toxicity. Combined administration exerted synergistic effects, disrupting the entire neuro-glio-vascular unit. Endothelial dysfunction emerged as the primary trigger. These findings underscore the multifactorial nature of CIPN and the need for early neuroprotective interventions targeting vascular stability and mitochondrial homeostasis. Basement membrane thickness increased from 158 $\pm$ 19 nm (day 14, paclitaxel group) to 268 $\pm$ 31 nm on day 28 in the combined treatment group.

**Key words:** chemotherapy-induced peripheral neuropathy, cisplatin, paclitaxel, sciatic nerve, ultrastructure, electron microscopy, rats.

**Г.Б. Кулинич, С.Б. Геращенко, В.М. Перцович, М.Д. Ризюк, І.Ю. Олійник, О.І. Тірон**

**ЕЛЕКТРОННО-МІКРОСКОПІЧНА ХАРАКТЕРИСТИКА ДИНАМІКИ УШКОДЖЕНЬ СІДНИЧНОГО НЕРВА ЩУРІВ ПРИ ЦІСПЛАТИН- І ПАКЛІТАКСЕЛ-ІНДУКОВАНІЙ НЕЙРОТОКСИЧНОСТІ**

Хіміотерапевтично індукована периферична нейропатія обмежує ефективність цисплатину та паклітакселу в лікуванні злойкісних пухлин. У цьому дослідженні охарактеризовано ультраструктурні зміни у сідничному нерві щурів на 14-ту та 28-му добу після введення препаратів із використанням трансмісійної електронної мікроскопії. Статевозрілих самців білих інbredних щурів (n=30 у кожній групі) розподілили на три групи: паклітаксел (2 мг/кг внутрішньоочеревинно, 4 ін'екції через день, сумарна доза 8 мг/кг), цисплатин (2 мг/кг внутрішньоочеревинно, двічі на тиждень протягом 4 тижнів, сумарна доза 16 мг/кг) та одночасне введення (цисплатин 2 мг/кг внутрішньоочеревинно при 37°C + паклітаксел 5 мг/кг внутрішньовенно раз на тиждень протягом 6 тижнів; сумарні дози: цисплатин 12 мг/кг, паклітаксел 30 мг/кг). Фрагменти нервів фіксували в 2% тетроксиді осмію, заливали в смоли Epon812/Araldite та досліджували при збільшенні  $\times 4800$ – $\times 16000$ . Цисплатин спричиняв більш виражену дегенерацію, ніж паклітаксел, включно з деструкцією міеліну, аксональною дегенерацією та набряком нейроглю-судинних комплексів. Вираженість ушкоджень посилювалася від 14-ї до 28-ї доби, що свідчить про кумулятивний характер токсичності. Комбіноване введення мало синергічний ефект, порушуючи структурну цілісність усього нейро-глю-судинного комплексу. Ендотеліальна дисфункція виявилася початковою ланкою патологічного каскаду. Отримані результати підкреслюють багатофакторну природу ХПН та необхідність раннього застосування нейропротекторних стратегій, спрямованих на стабілізацію судинної стінки та підтримання мітохондріального гомеостазу. Товщина базальної мембрани збільшувалася від 158 $\pm$ 19 нм (14-та доба, група паклітакселу) до 268 $\pm$ 31 нм на 28-му добу в групі комбінованого лікування.

**Ключові слова:** хіміотерапевтично індукована периферична нейропатія, цисплатин, паклітаксел, сідничний нерв, ультраструктура, електронна мікроскопія, щури.

*The study is a fragment of the research project "Morphofunctional changes in organs and body systems under the influence of antitumor drugs and under conditions of their correction", state registration No. 0121U111598.*

Chemotherapy-induced peripheral neuropathy (CIPN) is one of the most frequent dose-limiting toxicities associated with antitumor treatment and remains a major challenge in contemporary oncology. Cisplatin and paclitaxel, integral components of therapeutic regimens for many solid tumors, demonstrate well-documented neurotoxic potential that significantly affects patient functioning and quality of life. The sciatic nerve provides a robust experimental model for characterizing these processes because its neuroglio-vascular organization reflects the coordinated interactions of endothelial structures, Schwann cells, and axons. Increasing evidence suggests that CIPN develops through the interplay of endothelial dysfunction, mitochondrial damage, oxidative stress, and glial reactivity, forming a unified pathophysiological cascade [13, 15].

Paclitaxel disrupts axonal transport, destabilizes microtubules, and induces energetic failure in sensory neurons, leading to progressive axonal degeneration and segmental myelin injury [2, 14]. Cisplatin, in contrast, produces a pronounced vascular–endothelial pattern of neurotoxicity, characterized by thickening of the basement membrane, endothelial thinning, increased micropinocytosis, venular congestion, and secondary glial alterations [3, 8]. Both chemotherapeutic agents cause oxidative stress and mitochondrial impairment that compromise neurofilament integrity and weaken axonal resistance to metabolic overload [4, 9]. Although individual toxic effects of paclitaxel and cisplatin are well described, studies addressing their combined action remain limited, despite the fact that such regimens are widely applied in clinical oncology.

Recent conceptual models emphasize the neurogliovascular unit as an integrated target of chemotoxic injury. Endothelial disruption is increasingly viewed as an initiating event that precedes axonal degeneration and myelin fragmentation, creating conditions for cumulative and sustained neurotoxicity [1, 13]. Nevertheless, the temporal sequence of these events and the extent to which individual neurotoxic mechanisms interact under combined exposure require further clarification. Detailed ultrastructural and morphometric studies are crucial for understanding the progression of nerve injury and for defining structural targets for early neuroprotective intervention.

Given the growing interest in pharmacological agents capable of stabilizing mitochondrial function, reducing oxidative stress, or preserving endothelial integrity, establishing a precise morphological basis for CIPN is essential. Comparative ultrastructural studies can provide the foundation for developing rational strategies aimed at mitigating neurotoxicity during antitumor therapy.

**The purpose** of the study was to characterize and compare the temporal patterns of ultrastructural injury to the sciatic nerve following paclitaxel, cisplatin, and combined administration.

**Materials and methods.** The study was conducted on sexually mature male white inbred rats weighing 180–220 g at the beginning of the experiment. The animals were divided into three groups: Paclitaxel group (2 mg/kg intraperitoneally, four injections every other day, total dose – 8 mg/kg) – control group; Cisplatin group (2 mg/kg intraperitoneally, twice a week for four weeks, total dose – 16 mg/kg) – control group; and a combination group (experimental group) in which animals received both chemotherapeutic agents simultaneously: cisplatin at a dose of 2 mg/kg intraperitoneally (pre-warmed to 37 °C) and paclitaxel at a dose of 5 mg/kg intravenously via the tail vein once a week for six weeks (total of six injections; cumulative doses – cisplatin 12 mg/kg, paclitaxel 30 mg/kg). Each group included 30 animals.

All animals were bred in the vivarium of Ivano-Frankivsk National Medical University and housed under standard laboratory conditions (temperature 21±2 °C, humidity 55–60 %, 12 – hour light/dark cycle) with free access to water and food. Before the experiment, all animals underwent a 7-day adaptation period. Euthanasia was performed by inhalation of ether overdose. The experimental part of the study was conducted from late March to April 2025. Drug administration began on 02 April 2025. Sciatic nerve samples were collected on days 14 (16 April 2025) and 28 (30 April 2025) from the onset of chemotherapy, when the most pronounced ultrastructural changes were observed.

Sampling of the sciatic nerve was carried out on the 14th and 28th days after the start of drug administration. For electron microscopy, fragments of the lumbosacral spinal cord, spinal ganglia, and sciatic nerve segments approximately 1 mm<sup>3</sup> in size were collected. Fixation was performed by immersion in a 2 % aqueous solution of osmium tetroxide prepared in 0.1 M phosphate buffer (pH 7.4) for 2 hours. Samples were washed three times in fresh buffer of the same molarity for 30 minutes each.

Dehydration was carried out in a graded series of ethanol solutions (50 %, 70 %, 90 %, and 100 %). After preliminary staining with uranyl acetate, the samples were transferred into acetone and gradually infiltrated with mixtures of acetone and epoxy resins (Epon and Araldite) in ratios of 3:1, 1:1, and 1:3. Final embedding in epoxy resin was performed using a standard method, and polymerization of blocks containing oriented fragments was conducted at +56 C for 24 hours.

To verify tissue orientation, semithin sections were prepared and stained with methylene blue. Ultrathin sections were obtained using a UMTP-2M ultramicrotome, mounted on 1 mm copper grids, and stained with uranyl acetate and lead citrate. Examination was performed on a PEM-125K transmission electron microscope at magnifications of ×4800–×16000 with subsequent photodocumentation.

All manipulations were carried out in accordance with the European Convention for the Protection of Vertebrate Animals Used for Experimental and Other Scientific Purposes (Strasbourg, 1986) and the Helsinki Declaration (2013).

Morphometric analysis was performed using ImageJ 1.53k software (National Institutes of Health, USA). On electron micrographs of epineurial capillaries (magnification ×8600–×16000), the thickness of the

basement membrane was measured at ten random perpendicular intersections in each of 3–5 images per group and time point (30–50 measurements per group in total). Before measurement, the image scale was calibrated using the microscope's built-in scale bar. Results were expressed as mean  $\pm$  standard deviation (M $\pm$ SD) [12]. Statistical analysis was performed using one-way ANOVA followed by Tukey's post hoc test in GraphPad Prism 9.0 (GraphPad Software, USA). Differences were considered statistically significant at  $p < 0.05$ .

All procedures were carried out in accordance with the European Convention for the Protection of Vertebrate Animals Used for Experimental and Other Scientific Purposes (Strasbourg, 1986) and the Helsinki Declaration (2013). The study was approved by the Ethics Committee of Ivano-Frankivsk National Medical University (Protocol No. 146/24 dated 26 September 2024). All animals remained alive until the end of the experiment.

**Results of the study and their discussion.** Electron microscopy revealed marked and progressive alterations in the structure of the sciatic nerve following the administration of cisplatin and paclitaxel, demonstrating a distinct temporal pattern. By the 14th day of the experiment, early signs of toxic injury to the neurogliovascular complex were already evident, while by the 28th day, there was a well-defined picture of profound axonal destruction, vacuolization, demyelination, and vascular disorganization.

Structural abnormalities in the paclitaxel group were first evaluated on day 14 and day 28 (Fig. 1).

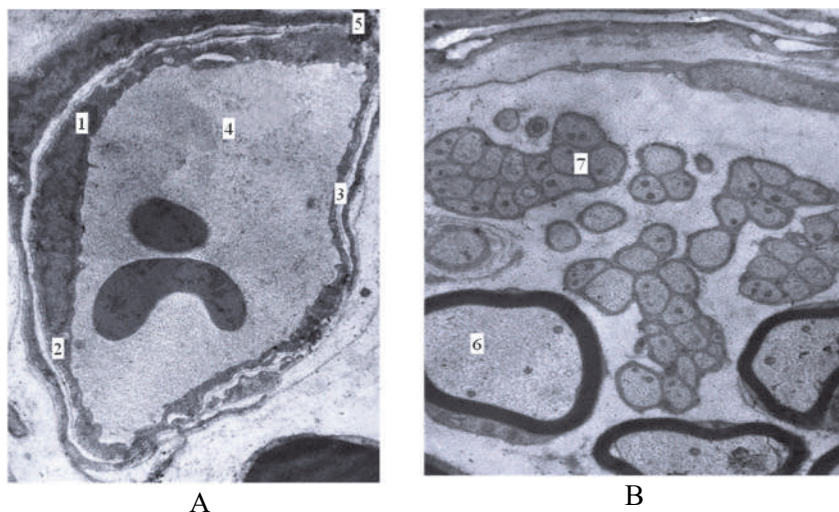


Fig. 1. Ultrastructure of the rat sciatic nerve in the paclitaxel group (a – 14th day after paclitaxel administration; b – 28th day after paclitaxel administration). Transmission electron micrographs. Magnification: (a)  $\times 3200$ , (b)  $\times 4800$ .

1 – endothelial cell; 2 – small vacuoles; 3 – basement membrane; 4 – capillary; 5 – pericyte; 6 – myelinated nerve fiber; 7 – unmyelinated nerve fiber.

Further assessment of the cisplatin group demonstrated a different injury pattern (Fig. 2).

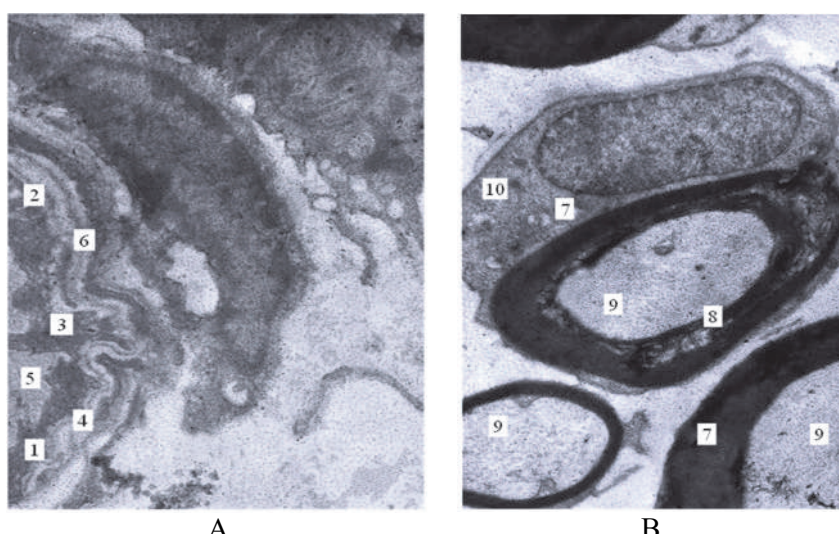


Fig. 2. Ultrastructure of the rat sciatic nerve in the cisplatin group (a – 14th day after cisplatin administration; b – 28th day after cisplatin administration). Transmission electron micrographs. Magnification: (a)  $\times 8600$ , (b)  $\times 6400$ .

1 – endothelium; 2 – vacuoles; 3 – micropinocytic vesicles; 4 – basement membrane; 5 – venue; 6 – pericyte; 7 – myelinated nerve fiber; 8 – intralamellar vacuoles; 9 – axonal cylinder; 10 – mitochondria.

A distinct thickening of the capillary basement membrane was found, together with cytoplasmic condensation of endothelial cells and narrowing of the vascular lumen. By day 28, dystrophic changes of moderate intensity were observed. Myelin sheaths displayed focal delamination, several axons contained vacuoles and swollen mitochondria, and the perivascular space was moderately enlarged while the perineurium remained intact. Occasional perineurial cells contained large vacuoles reflecting activation of autolytic processes.

On day 14, markedly dilated venules with congestion were present in the epineurium. The endothelium appeared thinned and contained numerous micropinocytic vesicles and vacuoles. Basement membranes were thickened, and pericyte processes were deformed and vacuolated. Adjacent Schwann cells exhibited cytoplasmic vacuolation and focal destruction. By day 28, profound destructive changes were identified: axonal cavitation, fragmentation of myelin lamellae into concentric bodies, disintegration of Schwann-cell cytoplasm, and thinning or deformation of

axonal cylinders. Small-diameter fibers remained relatively preserved, whereas medium- and large-diameter fibers showed intralamellar vacuoles and uneven separation of inner and outer myelin layers.

In the combined cisplatin + paclitaxel group (Fig. 3), the severity of damage exceeded that observed in either monotherapy group.

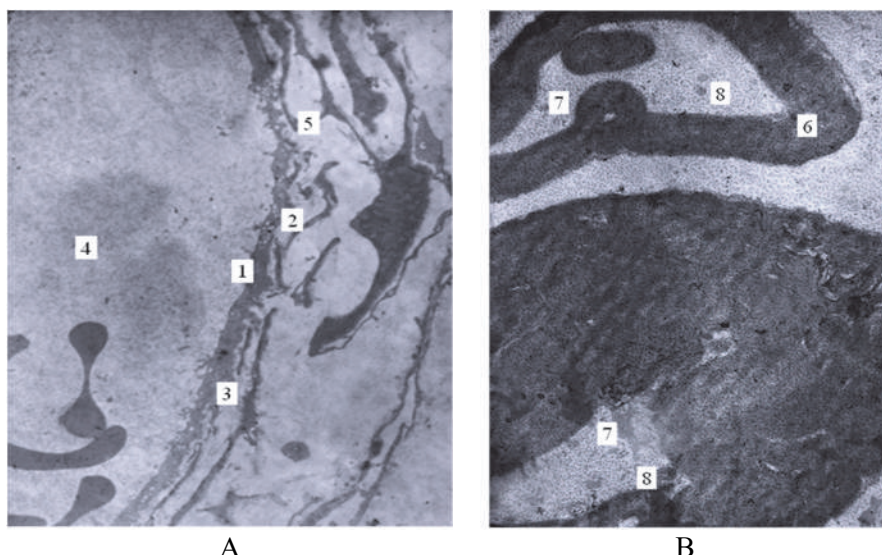


Fig. 3. Ultrastructure of the rat sciatic nerve in the cisplatin + paclitaxel group (a – 14th day after simultaneous administration of cisplatin and paclitaxel; b – 28th day after simultaneous administration of cisplatin and paclitaxel). Transmission electron micrographs. Magnification: (a)  $\times 4800$ , (b)  $\times 4800$ . 1 – endothelial cell; 2 – vacuoles; 3 – basement membrane; 4 – venule; 5 – pericyte; 6 – myelinated nerve fiber; 7 – axonal cylinder; 8 – mitochondria.

Morphometric analysis confirmed a statistically significant increase in the thickness of the capillary basement membrane in all experimental groups, with the greatest thickening recorded after combined drug administration. This parameter increased from moderately elevated values on day 14 to substantially higher levels by day 28, indicating progressive impairment of microvascular integrity. Overall, the morphological data demonstrate a consistent sequence of damage progressing from endothelial alterations to Schwann-cell injury, axonal degeneration, and myelin breakdown.

Morphometric analysis quantitatively confirmed the qualitative observations. In all experimental groups, a statistically significant increase in the thickness of the capillary basement membrane in the epineurium was observed, indicating the development of microvascular dysfunction. The most pronounced thickening was recorded in the group receiving the combined drug administration (Table 1).

Table 1

Thickness of the capillary basement membrane in the epineurium of the rat sciatic nerve (M $\pm$ SD, nm)

Group	Day 14 (nm)	Day 28 (nm)
Paclitaxel	158 $\pm$ 19	192 $\pm$ 23*
Cisplatin	178 $\pm$ 22	235 $\pm$ 28**
Combination	198 $\pm$ 25**	268 $\pm$ 31**

Notes: p<0.05; p<0.01 compared with the paclitaxel group at the corresponding time point (one-way ANOVA with Tukey's post hoc test, n = 40 measurements per group).

The obtained morphological data confirm that cisplatin and paclitaxel induce a sequential injury of the neurogliovascular complex, progressing from capillary endothelium to axonal structures. Early alterations exhibit a hypoxic-ischemic pattern (basement membrane thickening, luminal narrowing, cytoplasmic condensation), whereas late changes reflect cumulative toxicity, characterized by myelin destruction, axonal vacuolization, and mitochondrial degradation.

Thus, endothelial dysfunction represents the primary link in the formation of the neurogliovascular cascade, ultimately resulting in axonal degeneration. This highlights the potential of early pharmacological prevention aimed at stabilizing vascular endothelium and preserving glial and axonal integrity.

The obtained results can serve as a foundation for developing new approaches to the pharmacological prevention of neurotoxicity.

The study focuses on morphological and ultrastructural evaluation and therefore does not include functional parameters that could further clarify the relationship between structural alterations and the development of neurotoxicity. Certain discrepancies from clinical conditions may arise due to species-

On day 14, epineurial venules were markedly dilated and blood-engorged, the endothelium was thinned and actively formed transendothelial channels, and pericytes displayed dystrophic changes. By day 28, myelin sheaths were completely disorganized, with numerous concentric myelin figures. Axons were significantly thinned, and intralamellar vacuoles filled with amorphous material were prominent. Degenerated mitochondria and abundant profiles of neurotubules and neurofilaments were visible.

specific characteristics of the experimental model. These aspects form a basis for further expansion of the research.

The ultrastructural alterations identified in this study demonstrate that paclitaxel, cisplatin, and their combined administration produce a spectrum of damage to the neuroglioascular complex, consistent with the multifactorial mechanisms of CIPN. Early microvascular changes basement-membrane thickening, endothelial thinning, increased micropinocytosis, and venular congestion indicate that vascular dysfunction precedes neural degeneration. This concept aligns with the contemporary view that endothelial impairment represents an initiating step in the development of CIPN, disrupting perfusion and promoting hypoxic stress within peripheral nerves [3, 15].

The pattern of injury observed after paclitaxel administration reflects mechanisms described in experimental and clinical studies of taxane neurotoxicity. Microtubule destabilization, axonal vacuolization, and mitochondrial swelling correspond to the energetic failure and impaired axonal transport previously documented in preclinical models [1, 2, 7, 11, 14]. The vacuolization of Schwann cells seen in our material is consistent with glial susceptibility to paclitaxel-induced metabolic disturbances and altered glia-neuron interactions [8]. Similar adaptive and degenerative responses were also noted in studies evaluating paclitaxel-induced changes in other tissues, such as the oral cavity, emphasizing the systemic toxicity of this agent [10].

Cisplatin produced a distinct vascular-endothelial pattern of injury. Pronounced thickening of the basement membrane, luminal narrowing, and marked perivascular edema are characteristic features of cisplatin-induced microvascular dysfunction. These findings correspond to previously described mechanisms of endothelial compromise and inflammatory activation during platinum-based chemotherapy [3, 4, 15]. The concurrent mitochondrial and cytoplasmic alterations in Schwann cells observed here correlate with known cisplatin-induced oxidative and mitochondrial injury, which contribute to progressive demyelination and axonal degeneration [9, 14]. Similar injury patterns have been reported in experimental models of distal neuropathy, highlighting the generalizability of the cisplatin-damage cascade [5].

The most severe injury profile was recorded in the group receiving both cisplatin and paclitaxel. Complete myelin disorganization, concentric myelin figures, intralamellar vacuolization, and marked thinning of axonal cylinders indicate a cumulative and mutually potentiating effect on all components of the neuroglioascular complex. These synergistic effects are consistent with the amplified mitochondrial dysfunction and the impaired repair mechanisms described for combined chemotherapeutic exposure [8, 9, 14]. The sharp increase in basement-membrane thickness in this group further underscores the central role of endothelial failure in intensifying neural injury.

Our morphometric data confirm findings from studies that focus on structural quantification of myelinated fibers and capillary components. The observed increases in basement-membrane thickness align with prior methodological work demonstrating the importance of standardized morphometric criteria for assessing peripheral nerve injury [6]. The changes identified in medium- and large-diameter fibers correspond to established models of CIPN in which both axonal and myelin components are targeted [8, 14].

Certain parallels can also be drawn with neuropathic alterations observed in unrelated metabolic models, such as diabetic neuropathy, where glial swelling, basement-membrane thickening, and microvascular dysfunction similarly contribute to progressive neural degradation [12]. These similarities further support the concept that microcirculatory impairment and glial stress responses represent universal pathways in the evolution of peripheral neuropathies.

Overall, the present findings support the multifactorial model of CIPN pathogenesis, integrating microvascular dysfunction, glial reactivity, mitochondrial injury, cytoskeletal disruption, and cumulative toxic effects. The sequential progression from endothelial impairment to axonal degeneration highlights the neuroglioascular unit as an integrated target of chemotherapy-induced damage. This perspective underscores the rationale for early neuroprotective interventions aimed at stabilizing vascular integrity, supporting mitochondrial resilience, and preventing glial dysfunction [8, 15].

### Conclusion

Cisplatin and paclitaxel cause progressive, cumulative injury to the sciatic nerve: by day 14, microvascular and glial alterations predominate, whereas by day 28, profound axonal degeneration, demyelination, and mitochondrial destruction are observed.

Cisplatin acts mainly through a vascular-endothelial pathway, while paclitaxel targets axonal and glial structures; their combination produces a synergistic effect, leading to complete disorganization of the neuroglioascular complex.

Morphometric analysis confirmed a statistically significant increase in capillary basement membrane thickness - from  $158\pm19$  nm in the paclitaxel group to  $178\pm22$  nm (cisplatin) and  $198\pm25$  nm

(combination) on day 14, and up to 235±28 nm and 268±31 nm, respectively, on day 28 – quantitatively demonstrating the central role of endothelial dysfunction.

The data substantiate the need for early neuroprotection in oncology patients through endothelial stabilization and maintenance of mitochondrial homeostasis – representing a realistic strategy for preventing chemotherapy-induced peripheral neuropathy.

Further research should focus on evaluating the neuroprotective efficacy of pioglitazone and vortioxetine in models of cisplatin- and paclitaxel-induced neuropathy, supported by ultrastructural and morphometric analyses.

## References

1. Flatters SJL, Dougherty PM, Colvin LA. Clinical and preclinical perspectives on Chemotherapy-Induced Peripheral Neuropathy (CIPN): a narrative review. *Br J Anaesth.* 2017 Oct;119(4):737–49. DOI:10.1093/bja/aex229.
2. Fukuda Y, Li Y, Segal RA. A Mechanistic Understanding of Axon Degeneration in Chemotherapy-Induced Peripheral Neuropathy. *Front Neurosci.* 2017 Aug 31;11. DOI:10.3389/fnins.2017.00481.
3. Grisold W, Cavaletti G, Windebank AJ. Peripheral neuropathies from chemotherapeutics and targeted agents: diagnosis, treatment, and prevention. *Neuro Oncol.* 2012;14(4):iv45–54. DOI:10.1093/neuonc/nos203.
4. Joseph EK, Chen X, Bogen O, Levine JD. Oxaliplatin Acts on IB4-Positive Nociceptors to Induce an Oxidative Stress-Dependent Acute Painful Peripheral Neuropathy. *J Pain.* 2008 May;9(5):463–72. DOI:10.1016/j.jpain.2008.01.335.
5. Kotyvtska AA, Tykhanovych K V, Kryvoruchko TD, Neporada KS, Beregovyi SM. Paclitaxel-induced neuropathy induces changes in oral cavity organs of rats. *Regul Mech Biosyst.* 2023 Feb 7;14(1):102–5. DOI:10.15421/022315.
6. Kotyk T, Varkey TC, Demydchuk A, Shamalo S, Tokaruk N, Bedei V, et al. Morphometrical analysis of myelinated nerve fibers: is there a room for improvement? *Anat Sci Int.* 2025 Mar 10;100(2):191–7. DOI:10.1007/s12565-024-00801-6.
7. Li B, Jia S, Yue T, Yang L, Huang C, Verkhratsky A, et al. Biphasic Regulation of Caveolin-1 Gene Expression by Fluoxetine in Astrocytes: Opposite Effects of PI3K/AKT and MAPK/ERK Signaling Pathways on c-fos. *Front Cell Neurosci.* 2017 Oct 31;11. DOI:10.3389/fncel.2017.00335.
8. Mattar M, Umutoni F, Hassan MA, Wamburu MW, Turner R, Patton JS, et al. Chemotherapy-Induced Peripheral Neuropathy: A Recent Update on Pathophysiology and Treatment. *Life.* 2024;14(8):991. DOI:10.3390/LIFE14080991 Available from: <https://www.mdpi.com/2075-1729/14/8/991/htm>.
9. Melli G, Taiana M, Camozzi F, Triolo D, Podini P, Quattrini A, et al. Alpha-lipoic acid prevents mitochondrial damage and neurotoxicity in experimental chemotherapy neuropathy. *Exp Neurol.* 2008;214(2):276–84. DOI:10.1016/j.expneurol.2008.08.013.
10. Ostrovskyi M. Morphological manifestations of experimental paclitaxel-induced sciatic neuropathy under correction of 2-ethyl-6-methyl-3-hydroxypyridine succinate. *ScienceRise: Medical Science [Internet].* 2021;3(3(42)):20–6. DOI:10.15587/2519-4798.2021.232975 Available from: [https://journals.uran.ua/sr\\_med/article/view/232975](https://journals.uran.ua/sr_med/article/view/232975).
11. Takeuchi H, Jin S, Suzuki H, Doi Y, Liang J, Kawanokuchi J, et al. Blockade of microglial glutamate release protects against ischemic brain injury. *Exp Neurol.* 2008;214(1):144–6. DOI:10.1016/j.expneurol.2008.08.001.
12. Tykhanovych KV, Neporada KS, Yeroshenko GA. Pathomorphological changes in salivary glands of rats under the condition of diabetic neuropathy and correction. *World of Medicine and Biology.* 2023;19(83):229. DOI:10.26724/2079-8334-2023-1-83-229-232.
13. Vermeer CJC, Hiensch AE, Cleenewerk L, May AM, Eijkamp N. Neuro-immune interactions in paclitaxel-induced peripheral neuropathy. *Acta Oncol (Madr).* 2025;60(10):1369–82. DOI:10.1080/0284186X.2021.1954241 Available from: <https://www.tandfonline.com/doi/abs/10.1080/0284186X.2021.1954241>.
14. Xiao WH, Zheng H, Zheng FY, Nuydens R, Meert TF, Bennett GJ. Mitochondrial abnormality in sensory, but not motor, axons in paclitaxel-evoked painful peripheral neuropathy in the rat. *Neuroscience.* 2011 Dec;199:461–9. DOI:10.1016/j.neuroscience.2011.10.010.
15. Yamamoto S, Egashira N. Drug Repositioning for the Prevention and Treatment of Chemotherapy-Induced Peripheral Neuropathy: A Mechanism- and Screening-Based Strategy. *Front Pharmacol.* 2021 Jan 14;11. DOI:10.3389/fphar.2020.607780.

Стаття надійшла 19.10.2024 р.